*Journal of The Electrochemical Society*, **154** (3) J81-J85 (2007)
0013-4651/2007/154(3)/J81/5/$20.00 © The Electrochemical Society



# Transparent, Low Resistance, and Flexible Amorphous ZnO-Doped $In_2O_3$ Anode Grown on a PES Substrate

**Jung-Hyeok Bae,[a] Jong-Min Moon,[a] Jae-Wook Kang,[b] Hyung-Dol Park,[b] Jang-Joo Kim,[b] Woon Jo Cho,[c] and Han-Ki Kim[a,z]**

[a]*School of Advanced Materials and Systems Engineering, Kumoh National Institute of Technology, 1 Yangho-dong, Gumi, Gyeongbuk 730-701, Korea*
[b]*School of Materials Science and Engineering and Organic Light Emitting Diodes Center, Seoul National University, Silim-dong, Seoul 151-741, Korea*
[c]*Nano Device Research Center, Korea Institute of Science and Technology, 39-1 Haweolgok-Dong, Seongbuk-Gu, Seoul 136-791, Korea*

Transparent and low resistance amorphous ZnO-doped $In_2O_3$ (IZO) anode films were grown by radio-frequency (rf) sputtering on an organic passivated polyethersulfone (PES) substrate for use in flexible organic light-emitting diodes (OLEDs). Under optimized growth conditions, a sheet resistance of 15.2 Ω/□, average transmittance above 89% in the green range, and a root mean square roughness of 0.375 nm were obtained, even for the IZO anode film grown in a pure Ar ambient without the addition of oxygen as a reactive gas. All of the IZO anode films had an amorphous structure regardless of the rf power and the working pressure due to the low substrate temperature of 50°C and the structural stability of the amorphous IZO films. In addition, an X-ray photoelectron spectroscopy depth profile obtained for the IZO/PES showed no obvious evidence of interfacial reactions between the IZO anode and the PES substrate, except for some indiffusion of oxygen atoms from the IZO anode. Furthermore, the current-voltage-luminance of the flexible OLEDs fabricated on IZO anode was found to be critically dependent on the sheet resistance of the IZO anode.
 [DOI: 10.1149/1.2426800] 

Manuscript submitted August 25, 2006; revised manuscript received October 16, 2006. Available electronically January 10, 2007.

Flexible organic light-emitting diodes (OLEDs) are of considerable interest as the next generation displays, due to their lightweight, robust profile, ability to flex, curve, roll, and fold for portability, and ultimate engineering design freedom.[1-3] To obtain high-performance flexible OLEDs on a polymer substrate, producing high-quality anode films with a low resistivity, high transmittance, high work function, and stability to substrate bending is essential because device performance such as operating voltage, device stability and efficiency is critically affected by the carrier injection.[4] DC or radio-frequency (rf) sputter grown indium tin oxide (ITO) films are currently in widespread use in flexible OLED as the anode layer, due to their high conductivity and transparency in the visible spectral range.[5,6] However, an ITO anode, when grown at a low temperature to minimize thermal expansion of the polymer substrates has drawbacks, such as low conductivity and transmittance of amorphous ITO anode, chemical instability in a reduced ambient, the release of oxygen and indium into the organic layer, imperfect work function alignment with a typical hole transport layer (HTL).[7-10] Furthermore amorphous ITO films are easily transformed from amorphous to crystalline (a/c transform) at about 150°C, internal stress as a result of the a/c transformation leads to the severe cracking of ITO films.[11] Therefore, there has been a growing effort to develop TCO materials as substitutes for conventional ITO anode films. Amorphous IZO films are increasingly replacing conventional ITO films in the manufacture of flat panel displays as well as flexible displays.[12-16] Unlike amorphous ITO films, the low resistivity, high transparency, and excellent surface smoothness of amorphous IZO films can easily achieved by low-temperature sputtering without the need for reactive oxygen gas.[13,14] Therefore, it is generally thought that an amorphous IZO anode film is the best candidate for high-quality transparent conducting anodes in flexible displays. Ho et al., in an investigation of IZO anode films grown at ~50°C on a hard polycarbonate (HPC) substrate reported that a flexible OLED with an IZO anode showed a better performance than an OLED with a commercially available ITO anode film.[17] Hara et al., also reported that the resistivity of an amorphous IZO film grown on polycarbonate films decreased to $3 \times 10^{-4}$ Ω cm with increasing ZnO content above 5 wt %.[14] However, the characteristics of amorphous IZO anodes grown on thin film organic passivated polyethersulfone (PES) and the use of the IZO as an anode film in a phosphorescent flexible OLED has not been investigated in detail.

Therefore, in this work, we investigated the structural, electrical, optical, and surface properties of amorphous IZO films grown on a PES substrate in a pure Ar ambient as a function of rf power and working pressure. In addition, the a/c transformation temperature of amorphous IZO films was examined by X-ray diffraction (XRD) as a function of the rapid thermal annealing temperature. Furthermore, amorphous IZO anode films grown on PES substrates were employed as an anode in the fabrication of flexible OLEDs. It was shown that current-voltage-luminescence of the flexible OLEDs fabricated on an amorphous IZO anode is critically dependent on the sheet resistance of the amorphous IZO film.

## Experimental

120 nm-thick IZO anode films were sputtered on a PES substrate (*i*-component) by rf sputtering in a pure Ar ambient without the addition of reactive oxygen gas, which simplifies the deposition process. The PES substrate is hybrid passivated substrate (Organic layer/PES/$SiO_2$/Organic layer) with a transmittance of 90.8%, a water vapor transmission rate below 1 g/cm$^2$ day, and an oxygen transmission rate below 1 cm$^3$/m$^2$ day.[18] A specially designed 3 in. IZO target (5 wt % ZnO-doped $In_2O_3$, DNT Korea) was used as a ceramic target and was placed at a distance of 100 mm from the PES substrate. Base pressure of the system was maintained at $2 \times 10^{-6}$ Torr. At constant Ar flow rate (20 sccm) and a target to substrate distance of 100 mm, 120 nm-thick IZO films were grown on PES substrate with a dimension of 50 × 50 mm as a function of rf power and working pressure. To investigate the structural properties of an IZO film grown at optimized conditions, XRD, high-resolution electron microscopy (HREM), and transmission electron diffraction (TED) examinations were performed. In addition, to examine the a/c transformation temperature of the IZO films, amorphous IZO films intentionally grown on a glass substrate at optimized conditions were rapid thermally annealed in air up to 600°C and XRD examination was then carried out as a function of annealing temperature. The electrical properties of the IZO films were examined by Hall measurements at room temperature. The UV/vis transmittance of the IZO films and PES substrate was measured in wavelength range of 200 to 800 nm. The surface morphology of the IZO films was analyzed by scanning electron microscopy (SEM)

[z] E-mail: hkikim@kumoh.ac.kr

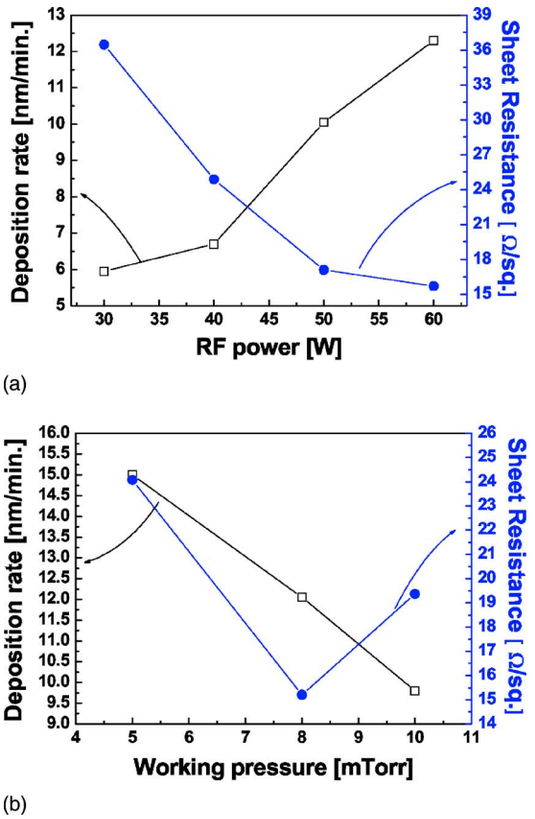


**Figure 1.** (Color online) Deposition rate and sheet resistance of an IZO anode grown on PES substrate as a function of (a) rf power and (b) working pressure, respectively.

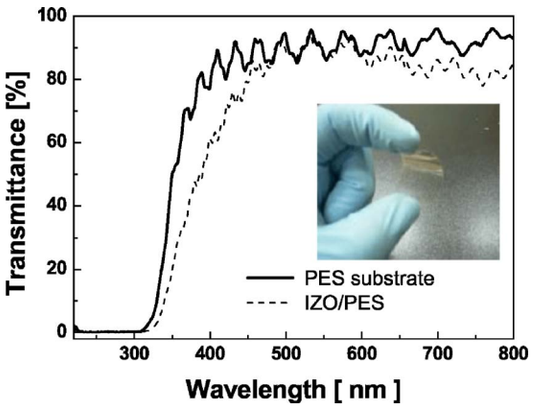


**Figure 2.** (Color online) Optical transmission spectra for IZO films deposited on a PES substrate and a bare PES substrate.

and atomic force microscopy (AFM). In addition, the binding energy of the IZO films was examined by XPS (PHI5200) using an Al Kα source in an ultrahigh vacuum system with a base pressure of $\sim 10^{-10}$ Torr. The XPS depth profile of IZO/PES was also performed to investigate interfacial reactions between the IZO and the PES substrate. To determine the effect of the sheet resistance of IZO anode films on density-voltage-luminescence (J-V-L) characteristics of flexible OLEDs, phosphorescent OLED were prepared with structures of Al/organiclayers/IZO/PES. All organic layers were grown on IZO anode films with different sheet resistance by thermal evaporation at $1 \times 10^{-7}$ Torr in the following order: hole transporting layer (HTL)/emission layer (EL)/hole blocking layer (HBL)/electron transporting layer (ETL)/electron injection layer (EIL) 40 nm thick α-napthylphenlylbiphenyl (NPB) and 30 nm thick 4,4′-bis(9-carbazolyl)-biphenyl (CBP) doped with 6 wt % [$Ir(ppy)_3$] were used as the HTL and EL, respectively. Subsequently, a 10 nm thick 2,9-dimethyl-4,7-diphenyl-1,10-phenanthroline (bathocuproine: BCP) layer was grown on the EL layer as a HBL layer. A 40 nm thick tris-(8-hydroxyquinoline)aluminum ($Alq_3$) ETL layer and a 1 nm LiF (EIL) layer were then deposited. Finally, a 100 nm thick Al cathode layer was patterned using a shadow metal mask. The current J-V-L characteristics of phosphorescent OLEDs fabricated on different anode materials were measured with a Keithely 2400 and a Si photodiode mounted below the OLEDs.

## Results and Discussion

Figure 1 shows the sheet resistance and deposition rate of the IZO films as a function of rf power and working pressure at a constant flow of pure Ar (20 sccm) and a working pressure of 8 mTorr to determine the optimum electrical properties of the IZO films. The sheet resistance of an IZO film with thickness of 120 nm dramatically decreased with an increase in RF power without heating the PES substrate in Fig. 1a. The minimum sheet resistance of 15.2 Ω/□ was obtained using an rf power of 60 W. The decrease in sheet resistance in the IZO films with increasing rf power can be attributed to the enhancement in kinetic energy of sputtered IZO atoms in the pure Ar ambient. Pan et al., investigating the influence of sputtering parameters on the optical and electrical properties of IZO, reported that the decrease in resistivity of IZO films with increasing rf power is related to an increase in the density of the IZO film and the elimination of phonon scattering and ionized impurity scattering.[18] Figure 1b shows the sheet resistance of IZO films as a function of working pressure at a constant Ar flow rate (20 sccm) and an rf power of 60 W. These data show that an increase in working pressure from 5 mTorr to 8 mTorr resulted in a decreased sheet resistance of IZO films. However, a further increase in working pressure led to an increase in sheet resistance of the IZO film due to the low kinetic energy of sputtered IZO atoms.

The optical transmittance of the IZO films grown at optimized conditions (60 W rf power and 8 mTorr) on PES substrates in the visible range is shown in Fig. 2 with the inset of the curved IZO/PES substrate. These findings clearly show that the transmittance of the IZO film is fairly high even though it was prepared at room temperature without oxygen reactive gas. Although the transmittance of the IZO film in the blue region is lower than that of the PES substrate, the average optical transmittance (89.1%) of the IZO anode in the green region between 500 and 550 nm is identical to that of a PES substrate (90.1%). To obtain transparent ITO anode films, an ITO film is generally grown at a high substrate temperature (200–300°C) under a flow of oxygen reactive gas. From the view of the process temperature for flexible OLEDs, IZO films with a high transmittance are the preferred TCO materials because they can simply be obtained at room temperature without the addition of reactive oxygen gas.

To investigate the structural properties of IZO films grown on a PES substrate in a pure Ar ambient, an XRD examination was carried out. Figure 3 shows XRD plots of IZO films as a function of rf power at a constant Ar flow rate (20 sccm), a working pressure of 8 mTorr, and a substrate to target distance of 100 mm. All XRD plots of the IZO films exhibit a broad peak ($2\theta = \sim 34°$), indicating a completely amorphous structure. The broad peak position is similar to diffraction peak of $In_2O_3$ (222), which is the component of an IZO film. XRD plots (not shown here) of the IZO films grown at different working pressure also show an amorphous structure at all working pressure ranges due to the low substrate temperature and the stability of IZO materials. The stability of the amorphous IZO phase below 500°C can be explained by the immiscibility of ZnO and $In_2O_3$.[1] For the crystallization of IZO films, phase separation of ZnO and $In_2O_3$ is required. During the phase separation of IZO, Zn

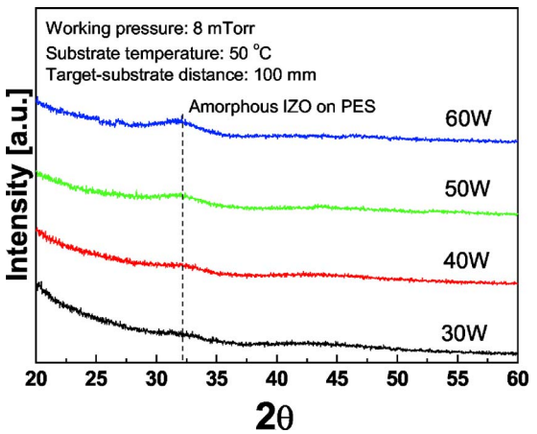


**Figure 3.** (Color online) XRD plot of IZO anode films grown on a PES substrate as a function of rf power.

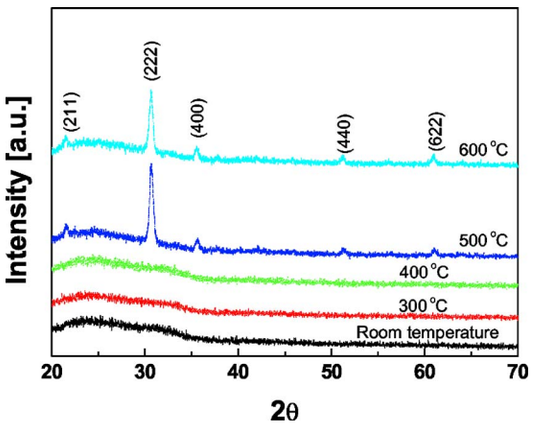


**Figure 5.** (Color online) XRD plot of IZO anode films grown on a glass substrate as a function of rapid thermal annealing temperature.

must be rejected from the crystallizing ITO structure. However, the kinetics of phase separation or Zn rejection are very low; as a result, the amorphous IZO can maintain a more stable amorphous structure than conventional ITO films.[1] Jung et al., investigating the influence of sputtering parameters on the properties of amorphous IZO films, also reported that crystallization temperature of an amorphous IZO film appears to be between 500 and 600°C, which was confirmed by differential thermal analysis (DTA).[19] Therefore, it is thought that the structural stability of the amorphous IZO films is beneficial for the stable performance of flexible OLEDs.

To investigate the microstructure of an amorphous IZO film grown on Si substrate at optimized conditions (60 W rf power, 8 mTorr), both HREM and TED examinations were employed. Figure 4 shows a HREM image obtained from the IZO film with an inset of a TED pattern obtained from IZO film. The uniform contrast of the IZO film indicates that the structure of the IZO anode films on Si substrate is completely amorphous, as expected from the XRD results. The TED patterns of all IZO films also exhibit a diffused ring pattern indicative of a completely amorphous structure. However, conventional ITO films prepared by dc or rf sputtering at room temperature had polycrystalline or amorphous structures with microcrystallines due to the low a/c transformation temperature.[11]

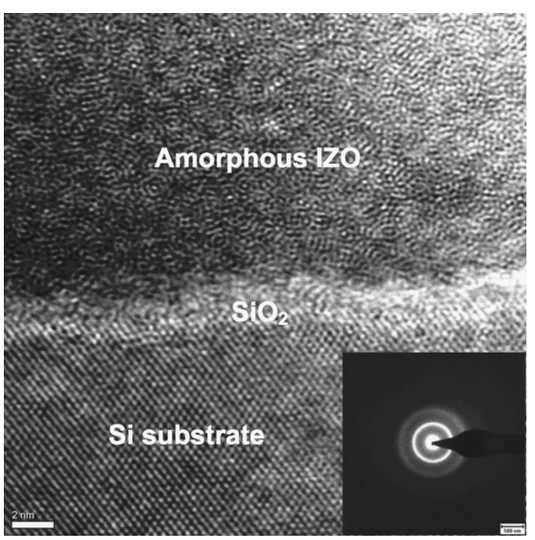


**Figure 4.** Cross-sectional HREM image obtained from an IZO anode layer grown on a Si substrate with the inset of a TED pattern.

Even if an ITO film is prepared at room temperature, crystallization occurs rapidly at low homogeneous temperatures ($T/T_m < 0.19$–$150$°C).[20,21]

To observe the a/c transformation temperature of an IZO film grown on a glass substrate in a pure Ar ambient, amorphous IZO films were intentionally prepared on glass substrates. The amorphous IZO/glass samples were then rapid thermally annealed in nitrogen ambient for 3 min. Figure 5 shows an XRD plot of the IZO films as a function of annealing temperature. No diffraction peak was observed below a temperature of 500°C. However, XRD plots of the 500- and 600°C annealed samples exhibit several peaks at $2\theta = 21.22°$ (211), 30.1° (222), 35.20° (400), 50.44° (440), and 60.22° (622), indicative of a crystalline structure. Although the temperature for a/c transformation is lower than reported data,[19] this confirms that the amorphous IZO films crystallized at a fairly high temperature due to the stability of the amorphous IZO structure.

The chemical binding state of the IZO films was investigated by XPS analysis as a function of rf power. Figure 6a-c shows the XPS peaks for O 1s, In 3d, and Zn 2p obtained for the IZO film as a function of rf power, respectively. As rf power is increased, no obvious change in the O 1s, In 3d, and Zn 2p peaks was observed. However, the lower binding peak in the O 1s peak obtained from an IZO film grown at 60 W rf power is higher that that obtained from an IZO film grown at 30 W rf power as shown in Fig. 4a. John et al. reported that two types of $O^{2-}$ ions, a lower binding energy peak ($O_{II}$) from the $O^{2-}$ ion have neighboring In atoms with their full complement and the higher binding energy peak ($O_I$) corresponds to oxygen-deficient regions.[22] Therefore, the decrease in higher binding peaks in O 1s peak indicates that the oxygen vacancies are decreased with increasing rf power due to the high density of the IZO film. Because the number of oxygen vacancies decreased with increasing rf power, the intensity of the higher binding energy peak decreased, consistent with the conclusion reported by John et al.[22]

Figure 7 shows the XPS depth profile obtained from the IZO/PES substrate sample. The IZO layer is well defined, indicating the absence of significant interfacial reactions between the IZO and the PES substrate due to the low substrate temperature. However, it is noteworthy that a small amount of oxygen atoms indiffused into the PES substrate. Although the PES substrate was passivated by organic layer, the less closely packed structure of organic passivation layer resulted in the indiffusion of oxygen atoms. Therefore, it would be desirable to passivate the both sides of the PES substrate with inorganic thin film to prevent the diffusion of oxygen atoms.

Figure 8 shows SEM and AFM surface images of an IZO film prepared at optimized conditions (60 W of rf power, 8 mTorr). Both images are very smooth and featureless without defects such as voids, cracks, and channels. The root mean square (rms) roughness

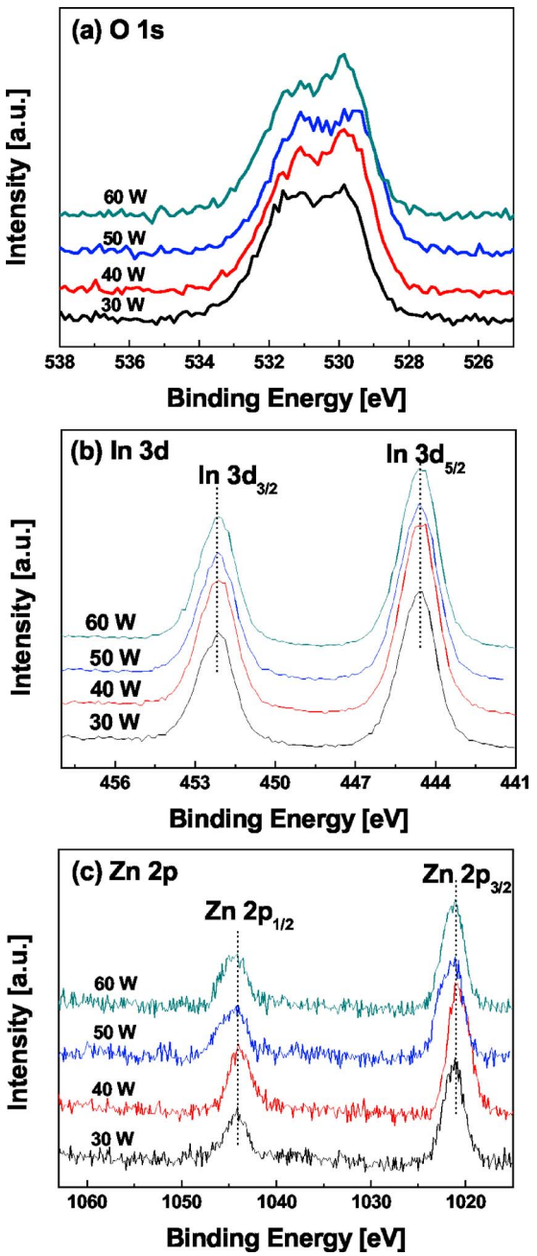


**Figure 6.** (Color online) XPS spectra of (a) O 1s, (b) In 3d, and (c) Zn 2p obtained for IZO anode films grown on a PES substrate as a function of rf power.

and peak-to-valley (PTV) values are 0.375 nm and 3.579 nm, obtained when the IZO film was grown at optimized conditions. These extremely low RMS roughness and PTV values indicate that IZO is a promising candidate for a substitute conventional ITO as the anode layer in flexible OLEDs. The smooth surface of the anode layer is very important in flexible OLEDs because excessive current can be generated by an anode film with a high PTV value.

Figure 9 shows the structure of a flexible OLED and the current density-voltage (J-V) characteristics of a flexible OLED fabricated on amorphous IZO anode films with different sheet resistance with the inset of luminance-current density plot. As shown in Fig. 9a, all of the organic layers were deposited on the side of PES substrate passivated by only organic layer. The outside of the PES substrate was passivated by inorganic($SiO_2$)/organic layer to prevent oxygen

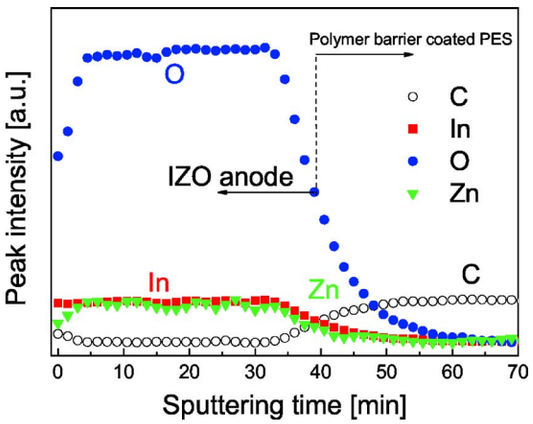


**Figure 7.** (Color online) XPS depth profile of IZO/PES substrate.

gas and moisture indiffusion from air though PES substrate. Even though both sides of the PES substrate were passivated by organic and inorganic/organic layers, the substrate shows high transmittance as shown in Fig. 3. Figure 9b shows that the flexible OLED fabricated on an IZO anode with a lower sheet resistance exhibits a lower turn on voltage and a higher current density. This indicates that the sheet resistance of anode layer critically affects the electrical properties of flexible OLEDs. The total resistance between A and B in Fig. 9a can be divided into four components: resistance of the metallic cathode $R_m$, resistance of organic layer $R_o$, resistance of the semiconducting IZO layer $R_{IZO}$, and contact resistance between each layer $R_c$. The contact resistance includes all interfaces such as cathode/organic, organic/organic, and organic/IZO contacts. Therefore the total resistance can be expressed as[23]

$$R_T = R_m + R_o + R_{IZO} + R_c \quad [1]$$

Because the resistance of the IZO anode layer is determined by the sheet resistance, the electrical characteristics of flexible OLED are also affected by the sheet resistance of the IZO anode layer. Although other resistance components, especially the contact resistance, critically influence the performance of flexible OLED, the correlation between the sheet resistance of the IZO and the J-V behavior of a flexible OLED shown in Fig. 9b suggest that the sheet resistance of the IZO anode also plays an important role in the performance of flexible OLEDs. As expected from the J-V curve, a flexible OLED with lower sheet resistance exhibits higher luminance at the same current density as shown inset of Fig. 9b. Because the J-V-L characteristics of an OLED strongly depends on not only the type of organic materials but OLED quality, a direct comparison of the J-V-L curve of a IZO based flexible OLED with a previous results is difficult.[17] However, good J-V-L characteristics of flexible OLED fabricated on the amorphous IZO anode indicate that the amorphous IZO anode is a promising candidate for a substitute for a conventional crystalline ITO anode for use in high-quality flexible displays.

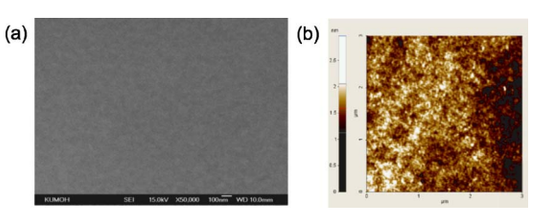


**Figure 8.** SEM and AFM surface images of the IZO anode film grown on PES substrate at optimized condition.

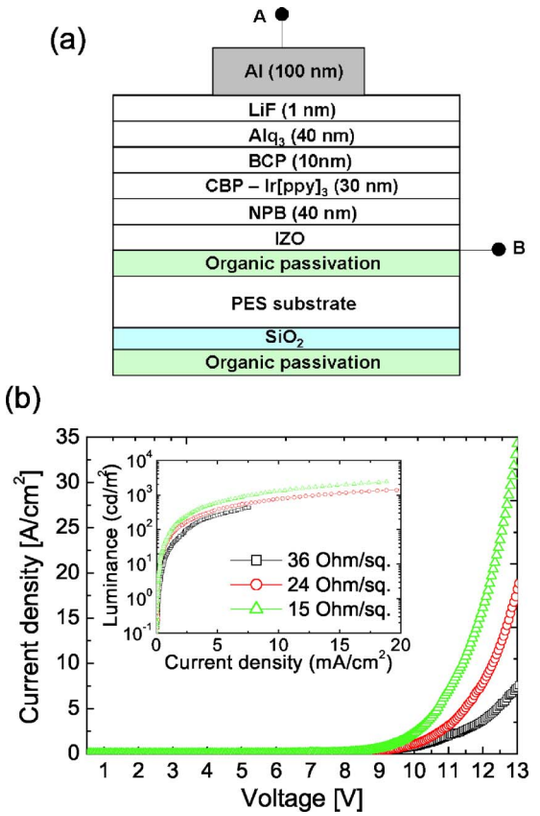


**Figure 9.** (a) Structure of a flexible OLED prepared on an IZO anode and (b) J-V-L characteristics of flexible OLEDs fabricated on an IZO anode with different sheet resistances.

## Conclusion

The characteristics of amorphous IZO anodes on PES substrate grown by rf sputtering for flexible OLEDs were investigated. At optimized growth conditions, a sheet resistance of 15.2 Ω/□, average transmittance above 89% in the green region, and a root mean square roughness of 0.375 nm were obtained even in the case of an IZO anode film grown in a pure Ar ambient without the addition of oxygen reactive gas. In addition, it was found that the crystallization temperature (~500°C) of an amorphous IZO film is higher than that (~150°C) of an ITO, due to the structural stability of the IZO film. It was found that no interfacial reactions occur at the region of interface between the IZO anode and the organic passivated PES substrate due to low substrate temperature. Furthermore, the J-V-L characteristics of the flexible OLEDs prepared on an IZO anode are critically affected by the sheet resistance of the IZO anode because the sheet resistance is one of the main components in total resistance of flexible OLED.

## Acknowledgments

This work was supported by a Korea Research Foundation grant funded by the Korean Government (MOEHRD: Basic Research Promotion Fund) (KRF-2006-003-D00243) and the Ministry of Commerce, Industry and Energy.

*Kumoh National Institute of Technology assisted in meeting the publication costs of this article.*

## References

1. Gregory P. Crawford, *Flexible Flat Panel Displays*, 1st ed., John Wiley & Sons, London (2005).
2. H. Lim, W.-J. Cho, C.-S. Ha, S. Ando, Y.-K. Kim, C.-H. Park, and K. Lee, *Adv. Mater. (Weinheim, Ger.)*, **14**, 1275 (2002).
3. K. Tsukagoshi, J. Tanabe, I. Yagi, K. Shigeto, K. Yanagisawa, and Y. Aoyagi, *J. Appl. Phys.*, **99**, 064506 (2006).
4. L. S. Hung and C. H. Chen, *Mater. Sci. Eng., R.*, **39**, 143 (2002).
5. J. Lewis, S. Grego, B. Chalamala, E. Vick, and D. Temple, *Appl. Phys. Lett.*, **85**, 3450 (2004).
6. H. Han, D. Adams, J. W. Mayer, and T. L. Alford, *J. Appl. Phys.*, **98**, 083705 (2005).
7. J. Cui, A. Wang, N. L. Edleman, J. Ni, P. Lee, N. R. Armstrong, and T. Marks, *Adv. Mater. (Weinheim, Ger.)*, **13**, 1476 (2001).
8. A. R. Schlatmann, D. W. Floet, A. Hillberer, F. Garten, P. J. M. Smulders, T. M. Klapwijk, and G. Hadziioannou, *Appl. Phys. Lett.*, **69**, 1764 (1996).
9. Y. Park, V. Choong, Y. Gao, B. R. Hsieh, and C. W. Tang, *Appl. Phys. Lett.*, **68**, 2699 (1996).
10. J. M. Philips, J. Kwo, G. A. Thomas, S. A. Carter, R. J. Cava, S. Y. Hou, J. J. Krajewski, J. H. Marshall, W. F. Peck, D. H. Rapkine, and R. B. V. Dover, *Appl. Phys. Lett.*, **65**, 115 (1994).
11. Y. Shigesato, D. C. Paine, and T. E. Haynes, *Adv. Mater. (Weinheim, Ger.)*, **4**, 503 (1994).
12. T. Minami, H. Sonohara, T. Kakumu, and S. Takata, *Jpn. J. Appl. Phys., Part 1*, **34**, 971 (1995).
13. T. Minami, T. Kakumu, and S. Takata, *J. Vac. Sci. Technol. A*, **14**, 1704 (1996).
14. H. Hara, T. Hanada, T. Shiro, and T. Yatabe, *J. Vac. Sci. Technol. A*, **22**, 1726 (2004).
15. A. Sugimoto, H. Ochi, S. Fujimura, A. Yoshida, T. Miyadera, and M. Tsuchida, *IEEE J. Sel. Top. Quantum Electron.*, **10**, 107 (2004).
16. C. Marcel, N. Naghavi, G. Couturier, J. Salardenne, and J. M. Tarascon, *J. Appl. Phys.*, **91**, 4291 (2002).
17. J.-J. Ho and C.-Y. Chen, *J. Electrochem. Soc.*, **152**, G57 (2005).
18. H.-C. Pan, M.-H. Shiao, C.-Y. Su, and C.-N. Hsiao, *J. Vac. Sci. Technol. A*, **23**, 1187 (2005).
19. Y. S. Jung, J. Y. Seo, D. W. Lee, and D. Y. Jeon, *Thin Solid Films*, **445**, 63 (2003).
20. Y. Shigesato, S. Takaki, and T. Haranoh, *J. Appl. Phys.*, **71**, 3356 (1992).
21. T. Oyama, *J. Vac. Sci. Technol. A*, **10**, 1682 (1992).
22. J. C. C. Fan and J. B. Goodenough, *J. Appl. Phys.*, **48**, 3524 (1977).
23. D. K. Schroder, *Semiconductor Material and Device Characterization*, 2nd ed., John Wiley & Sons, New York (1998).